Uniport Journal of Engineering and Scientific Research (UJESR)

Vol. 8, Issue 2, 2024, Page 283-296
ISSN: 2616-1192

(www.ujesr.org)

Exergy And Exergoeconomic Analysis of a Developed Small-Scale Waste Plastics Pyrolysis Plant for Diesel Oil Recovery from Thermoplastics

Igwe, J.E[1]*, Ashimedua, O.G[2], Okoro U.I[1], Igboayaka, E.C[1] and Mba, B.C[1]
[1]Mechanical Engineering department, Michael Okpara University of Agriculture Umudike
[2]Delta State Polytechnic, Ogwashi-Uku, Nigeria.
*Corresponding author's email: igwe.johnson@mouau.edu.ng

Abstract
The exergy and exergoeconomics analysis on a developed small-scale waste plastic pyrolysis plant for diesel oil recovery from thermoplastics has been completed. The exergy and exergoeconomics analysis were applied to the four components of the plant: the reactor, catalytic cracker, diffuser, and air-condenser to identify Components with higher exergy destruction and cost-related improvements in the system. The readings obtained during the experimental investigation were fitted on the exergoeconomics model equations and they were simulated with engineering equation software (EES). The results indicated that the reactor component has the highest value of exergy destruction of 0.4322 (kW). Furthermore, the exergoeconomics analysis revealed improvement of the condenser due to its low exergoeconomics factor of 0.00261 and high total cost rate of 1.895 $/h. However, the condenser will be improved if the investment cost rate and exergy destruction can be reduced.

Keywords: *Waste plastics, Pyrolysis plant, Diesel oil, Exergy, Exergoeconomics analysis*

Received: 24th September, 2024 *Accepted: 31st December, 2024*

1. Introduction

Exergy is the maximum work obtained in a reversible system interacting with the environment to attain equilibrium, considering the environmental parameters (such as temperature and pressure) as the reference state (Kelly *et al.,* 2009). Exergy analysis is important in identifying and quantifying both the consumption of useful energy (exergy) used to drive a process as well as the irreversibilities (exergy destruction) and the losses of exergy. It also reveals the areas of inefficiencies. Exergy analysis can highlight the areas of improvement in a system (Morosuk and Tsatsaronis 2015). The exergoeconomic costs stand for the monetary costs of streams of matter and energy flows. The exergoeconomics analysis reveals the components of higher cost due to the increase of exergy destruction or cost of materials in the system (Vuckovic *et al.,* 2012).

The exergy and exergoeconomics analysis identify components and their corresponding parameters that must be enhanced to achieve an optimum system configuration (Kelly *et al.,* 2009).
Eugene (2013) introduced a model for switchgrass production and its conversion to bio-oil utilizing fast pyrolysis. Switchgrass is a primary energy crop due to its high biomass yield in an assortment of soil conditions. The energy and exergy reproducing factors were 18.9 and 2.3 respectively.

Ryan (2015) investigated the simulation of the waste tire pyrolysis process in ASPEN Plus® 8.4, where the impact of temperature on the pyrolytic oil yield was explored. The exploration shows that the ideal temperature for waste tire pyrolysis in a revolving furnace reactor is around 450-550ºC. The generally exergetic productivity of the reactor was discovered to be 69.9% which is identical to exergy destruction of 30.1% because of process irreversibility. But the exergoeconomics analysis was not conducted to know the component with high cost of maintenance.

Jens *et al.* (2015) presented an exergetic examination of a quick pyrolysis plant recreated in Aspen Plus, producing rough bio-oil from lignocellulosic feedstock (crossover poplar woodchips). The sizeable exergetic productivity of the plant is discovered to be 71.2%, with the gas-and-singe combustor of the plant causing the most noteworthy exergy destruction. The exergoeconomics analysis of the pyrolysis plant was not considered.

Rashad and Maihy (2009) performed an energy and exergy analysis of a steam power plant in Egypt. As a result, the percentage ratio of the exergy destruction to the total exergy destruction was found to be maximum in the turbine system (42% at maximum load, 59% at 75% load and 46.9% at 50% load), followed by the condenser (28% at maximum load, 20.3% at 75% load) while at 50% load the feedwater heaters showed more exergy destruction (27%) than condenser which stood at 23.8%. The component cost analysis of the pyrolysis plant was not considered.

Mehrpooya *et al.* (2016) investigated a mechanical refrigeration cycle with propane refrigerant using a high-level exergy examination technique. The exergetic productivity of the refrigeration cycle was resolved to be 33.9%, indicating a high potential for improvements. The cost related exergy stream of the pyrolysis plant was not done.

Açıkkalp *et al.* (2014) evaluated the high-level exergy investigation of a power-creating office utilizing petroleum gas. The exergy efficiency of the framework was resolved to be 40.2%, while the absolute exergy destruction of the framework was determined to be 78.242 MW.

Erbay and Hepbasli (2014) introduced a high-level exergy investigation applied to a ground-source heat siphon (GSHP) drying framework utilized in food drying for evaluating its exhibition alongside every component. The conventional and changed (progressed) exergy effectiveness esteems were determined to be 77.05% and 93.5%, individually.

Kelly *et al.* (2009) further described the method for splitting exergy destruction into exogenous and endogenous parts, illustrating the component irreversibilities. The avoidable exergy destruction recorded in the combustion chamber is 35.05MW which deviated from the result obtained by other authors (28.54MW). But their work did not consider exergoeconomics analysis to identifies component with high cost of energy.

There is need to know the areas of improvement in terms of exergy destruction of the component and the component with higher cost of energy in the pyrolysis plant for diesel oil production in Mouau. So, the following objectives were considered: to perform exergy analysis of the waste plastics pyrolysis plant, to carry out exergoeconomics models of the entire plant components, and to conduct sensitivity analysis of the plant.

2. Materials and methods

2.1 Materials

The materials used for the work include two (2) kg of Mixed Waste Plastics (Thermoplastics): Polyethylene (PE), Polypropylene (PP), and Polystyrene (PS) (Rajendra 2017). One (1.0) kg of iron catalyst was used in the reactor. The ratio of waste plastics to catalyst is 2:1 inside the reactor component during pilot test. The data used in the analysis of the waste plastics pyrolysis plant were obtained from the pilot test of each batch operation of the plant. The software used was Engineering Solver (EES) for the simulation of the exergy and exergoeconomics equations.

2.1.1 Parts of waste plastics plant and their description

The waste plastics pyrolysis plant components are the reactor, catalytic cracker, diffuser, air-condenser, and oil collector. The reactor is the main part of the pyrolysis plant. The raw materials (mixed waste plastics) and catalysts (iron) are fed into the reactor. It melts the plastics and converts them to vapour at high temperatures. The catalytic cracker contains a catalyst (mixture of quartz sand and FCC) in the chamber. It degrades the waste plastic vapour at high temperatures as a vapour bath or flows into the chamber. The diffuser component regulates the fluid flow rate entering the air condenser. The air-condenser component condensed the vapour to liquid oil. The condensed oil from the condenser flows to the oil collector.

2.2 Methods

2.2.1 Principle of operations

The schematic of the waste plastic pyrolysis plant is shown in Fig.1., and the 3D drawing of the waste plastics plant is represented in Fig. 2. The production method for the conversion of plastics to liquid fuel is based on the pyrolysis of the plastics and the condensation of the resulting hydrocarbons. The plastic waste was first shredded into sizes and removed from any moisture content. The mixture of waste plastics and catalysts (quartz sand and iron) was then introduced into the reactor to enhance the degradation of oil vapour from higher molecular weight to lower molecular weight and is called the primary cracking process. The waste plastics were heated and melted at a temperature range of 150-180^{0}C. The melted liquid plastics were decomposed or vaporized at an inlet reactor temperature range of 250 – 500 ^{o}C, at point 1, in the thermodynamics state point, and evaporate at point 2, at the state point. The vaporized oil was subjected to the

catalytic cracker's secondary cracking process at points 3 and 4. The vaporized oil vapour was also degraded due to the impact on the catalyst (quartz sand and iron chips) at elevated temperatures. The flow rate of the light oil was reduced or dropped in the diffuser to enable the fluid to spend more time in the condenser for condensation to occur at points 5 and 6. The waste plastic vapour was condensed in the air-cool condenser. The heat from the waste plastic vapour was rejected by the surroundings at points 7 and 8. The blowing fan channels a steady flowing air to the condenser to remove heat from the oil gas between points 9 and 10. The liquid hydrocarbons were then collected in a storage tank. Gaseous hydrocarbons such as methane, ethane, propylene, and butanes cannot be condensed and were therefore incinerated in a flare stack or stalled for cooking gas purposes.

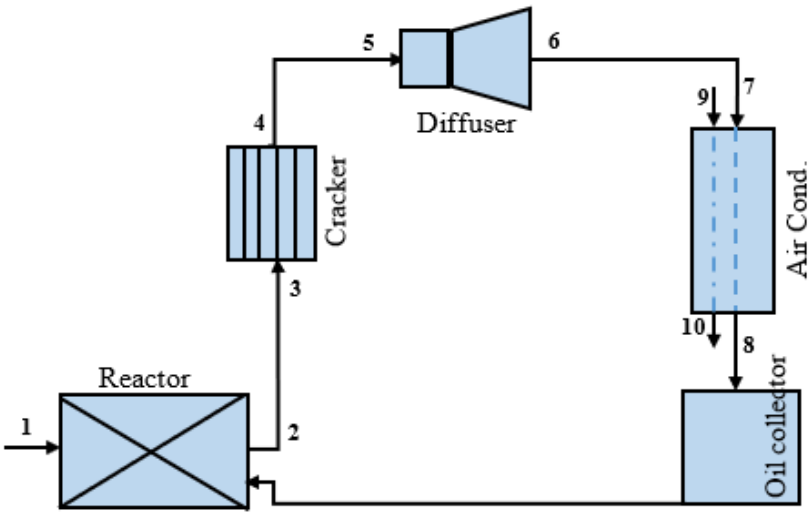

Fig.1: The waste plastics pyrolysis energy plant

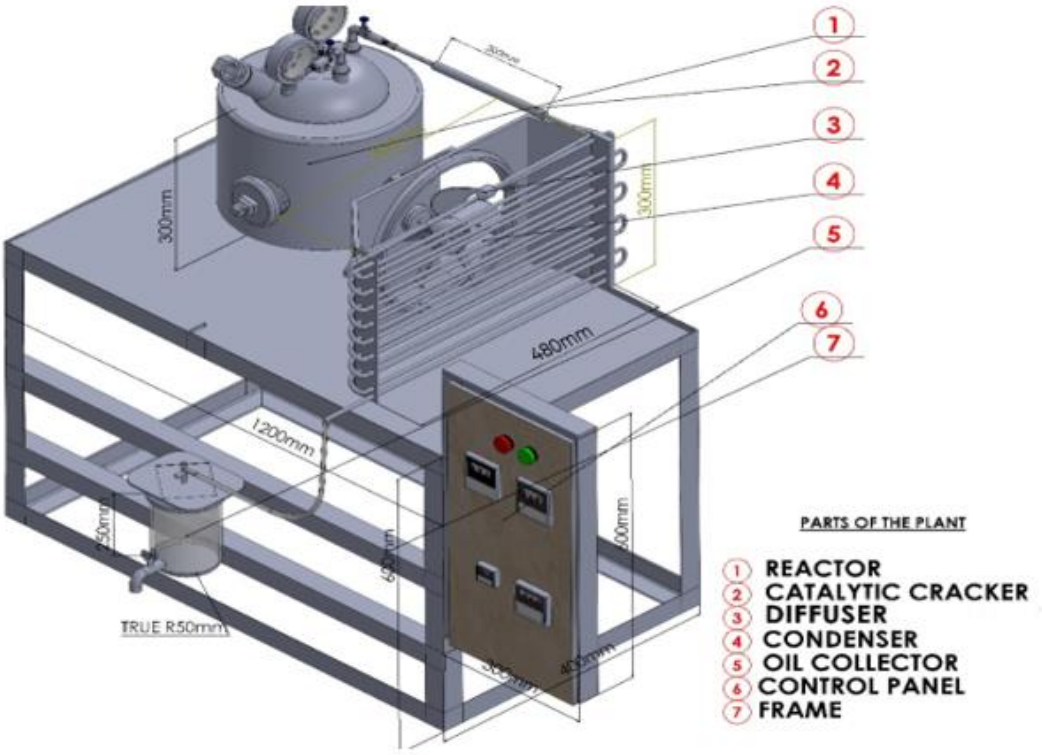

Fig. 2: The 3D drawing of the waste plastics pyrolysis plant

2.2.2 Experimental procedure of waste plastics pyrolysis plant

The pilot test of the waste plastic pyrolysis plant in the Michael Okpara University of Agriculture Umudike was carried out using shredded 2 kg of mixed waste plastics (PP, PE, and PS), measured in the weighing machine. The empty reactor was also measured in the weighing machine. 2 kg of mixed waste plastics and 1.0 kg of catalyst were fed inside the reactor and weighed in the weighing machine. Thermocouples were fitted at the reactor base to regulate inlet temperature from the 3kW heater placed at the bottom of the reactor. The inlet reactor temperatures used to produce one liter of petroleum products were in the range of 310, 360, 400, 460, and 500ºC at the residence time of 60, 54, 50, 46, and 43 minutes, respectively. The waste plastics pyrolysis plant was powered electrically to produce five different samples of liquid products, and the oil samples were taken to the Principal Laboratory Technologist at the National Root Crops Research Institute Umudike for characterization. The reactor was finally weighed in the weighing machine after the experiment.

2.3 The exergy analysis of the pyrolysis plant

The concept of exergy is used here to quantify the streams' relative heat and work rate concerning the thermodynamic irreversibilities in the system. The expressions that define the energy and exergy streams for a steady-state process are presented in Equations (1) and (2), respectively, as (Morosuk and Tsatsaronis, 2015; Mosaffa *et al.*, 2014).

$$\sum \dot{Q}_k + \sum \dot{m}_i \left(h_1 + \frac{C_i^2}{2} + g9z_1\right) = \sum \dot{m}_i \left(h_0 + \frac{C_0^2}{2} + gz_0\right) + \sum \dot{W} \quad (1)$$

$$\sum \left(1 + \frac{T_0}{T}\right) \dot{Q}_k + \sum(\dot{m}_i \varphi_i) = \sum \varphi w + \sum(\dot{m}_0 \dot{\varphi}_0) + \dot{E}_D \quad (2)$$

Neglecting the kinetic and potential energies, the mass, energy, and exergy balances respectively for the equilibrium state can be expressed in Equation (3).

$$\sum \dot{m}_i = \sum \dot{m}_0 \quad (3)$$

$$\dot{Q} - \dot{W} = \sum \dot{m}_0 h_0 - \sum \dot{m}_i h_i \quad (4)$$

$$\dot{W} + \sum(\dot{m}_i e_i) = \dot{Q} + \sum(\dot{m}_0 e_0) \quad (5)$$

The rate of exergy transfer by heat E_Q at temperature T (K), specific exergy, and the overall exergy flow are expressed in Equations (6), (7), and (8):

$$E_Q = Q\left(1 - \frac{T_0}{T}\right) \quad (6)$$

$$e = \{(h - h_0) - T_0(s - s_0)\} \quad (7)$$

$$\dot{E} = \dot{m}e = \dot{m}\{(h - h_0) - T_0(s - s_0)\} \quad (8)$$

where h_0 (kJ/kg) and s_0 (kJ/kg-K) are specific enthalpy and entropy, both defined at dead state pressure and temperature P_0 (bar) and T_0 (K), respectively. The expressions in equations (3), (4), and (5) helped develop the component exergy balances as well as component exergy efficiencies as depicted in the following expressions:

The exergy balance in the reactor

The exergy balance in the reactor (Koroglu and Sogut, 2017) is represented in Equation (9)

$$\dot{E}_Q + \dot{E}_1 = \dot{E}_2 + \dot{E}_{D_{re}} \quad (9)$$

The exergy efficiency for the reactor

The exergy efficiency for the reactor (Lazzaretto and Tsatsaronis, 2006) is stated in Equation (10)

$$\varepsilon_{re} = \frac{\dot{E}_2}{\dot{E}_{1+}\dot{E}_Q} \quad (10)$$

The cracker exergy balance

The cracker exergy balance (Mosaffa, 2014) is indicated in Equation (11)

$$\dot{E}_3 = \dot{E}_4 + \dot{E}_{D_{Cr}} \quad (11)$$

The exergy efficiency of the cracker

The exergy efficiency for the cracker (Rashad and El-Maihy, 2009) is stated in Equation (12).

$$\varepsilon_{cr} = \frac{\dot{E}_4}{\dot{E}_3} \quad (12)$$

Diffuser exergy balance

The exergy balance in the diffuser (Ryan, 2015) is expressed with the relationship, stated in Equation (13).

$$\dot{E}_5 = \dot{E}_6 + \dot{E}_{D_{dif}} \quad (13)$$

Exergy efficiency for the diffuser

The exergy efficiency for the diffuser (Abam *et al.*, 2012) is expressed with the relationship stated in Equation (14).

$$\varepsilon_{dif} = \frac{\dot{E}_6}{\dot{E}_5} \quad (14)$$

Air condenser exergy balance

The air condenser exergy balance (Morosuk *et al.*, 2013) is given in Equation (15)

$$\dot{E}_7 + \dot{E}_9 = \dot{E}_8 + \dot{E}_{10} + \dot{E}_{D_{cd}} \quad (15)$$

Exergy efficiency for the air-condenser:

The exergy efficiency for the air-condenser (Mosaffa *et al* 2014) is indicated in Equation (16).

$$\varepsilon_{cd} = \frac{\dot{E}_{10} - \dot{E}_9}{\dot{E}_7 - \dot{E}_8} \quad (16)$$

The overall exergy balance, the exergy of fuel, and the exergy of the product for the system components analysis are summarised in Table 1.

Table 1: Summary of the exergy balance, exergy of fuel, and exergy of product

Component	Exergy balance	Exergy of fuel	exergy of product
Reactor	$\dot{E}_Q + \dot{E}_1 = \dot{E}_2 + \dot{E}_{D_{re}}$	$\dot{E}_Q + \dot{E}_1$	$\dot{E}_2$
Cracker	$\dot{E}_3 = \dot{E}_4 + \dot{E}_{D_{Cr}}$	$\dot{E}_3$	$\dot{E}_4$
Diffuser	$\dot{E}_5 = \dot{E}_6 + \dot{E}_{D_{dif}}$	$\dot{E}_5$	$\dot{E}_6$
Air condenser	$\dot{E}_7 + \dot{E}_9 = \dot{E}_8 + \dot{E}_{10} + \dot{E}_{D_{cd}}$	$\dot{E}_7 + \dot{E}_9$	$\dot{E}_{10} + \dot{E}_8$

2.4 Exergoeconomic analysis of the pyrolysis plant

The concept of exergoeconomics analysis is used to assess the techno-economic performance based on an exergy basis and determine the cost per unit exergy of the system's products (Bejan *et al.*, 1996). For any system receiving heat Q, and performing some work, W with the influx E_i and exergy efflux E_e, a general cost can be written as (Lazzaretto and Tsatsaronis, 2006) as seen in Equation (17)

$$c_{q,k}E_{q,K} + \sum_i \left(c_i \dot{E}_\iota\right)_k + \dot{Z}_K = \sum_e \left(c_e \dot{E}_e\right)_k + c_{w,k}\dot{W}_k \quad (17)$$

where $\sum_e \left(c_e \dot{E}_e\right)_k$ is the cost rates associated with exit exergy streams of the ***k*th** component, $c_{w,k}\dot{W}_k$ is the cost rate of power generation, $c_{q,k}\dot{E}_{q,k}$ is the cost rates related to heat transfer, $\sum_i \left(c_i \dot{E}_\iota\right)_k$ is the cost rates associated with entering exergy streams, $\dot{Z}_k$ is the capital investment cost rate, while c_e, c_w, c_q, c_i are the average costs per unit of exergy. In the absence of heat and work interactions, the exergoeconomic balance is reduced to the form seen in Equation (18).

$$\sum_i \left(c_i \dot{E}_\iota\right)_k + \dot{Z}_K = \sum_e \left(c_e \dot{E}_e\right)_k \quad (18)$$

Alternatively, using the concept of "exergy of product" and "exergy of fuel" (Lazzaretto and Tsatsaronis, 2006), the exergoeconomic balance at the component level can be written in the form stated in Equation (2.19).

$$c_F \dot{E}_F + \dot{Z} = c_P \dot{E}_P \quad (19)$$

The total cost rates in component ($\dot{Z}_k$) are associated with the capital investment ($\dot{Z}_{cl}$) , and the operation maintenance ($\dot{Z}_{om}$) cost rate of that component (Mortazavi and Mehran, 2017) is similarly represented in Equation (20).

$$\dot{Z}_k = \dot{Z}_{cl} + \dot{Z}_{om} \quad (20)$$

The calculation procedure for obtaining cost balance at the component level is fully described in (Darabi et al 2015) and uses the F-rule and P-rule. Other cost balances for the plant components are presented in the subsequent subsections.

2.4.1 Cost rates of the plant components

In the exergoeconomics analysis of energy systems, the cost rates of the plant components are usually modelled concerning the system's operating parameters in monetary units. Thus, each of the rates is a function of the purchased, equipment cost and the number of hours of plant operation, levelised in monetary units (Açıkkalp *et al.*, 2014) with the relationship expressed in the Equation (21).

$$\dot{Z}_k[\$/hr.] = \frac{\phi_k . \dot{C}_K}{N} \quad (21)$$

The maintenance factor for each plant component whose expected life is N years, and $\dot{C}_K$ is the annual levelised cost. Then, in line with the expression for present worth factor (PWF) of capital investment, $\dot{C}_K$ it is expressed with the relationship (Gorji-Bandpy *et al.*, 2010) as indicated in Equation (22).

$$C_k\ [\$/hr.] = [PEC - (SV)\ PWF(i,n)]CRF(i,n) \quad (22)$$

where PEC is the purchase of equipment cost, the capital recovery factor, CRF, is obtained in Equation (23).

$$CRF = \frac{i(1+i)^n}{[(1+i)^n - 1]} \quad (23)$$

SV represent the salvage value, while the present worth factor PWF is obtained with the relationship below as stated in Equation (24).

$$PWF = (1+i)^{-n} \quad (24)$$

In the considered system, the components already have standard cost rates. Therefore, the use of purchase and equipment cost to be levelized will not be viable. However, the individual cost balances will suffice in determining the cost rates at the state points.

Reactor cost balance

The cost balance for the reactor (Trinadade *et al.*, 2008) is expressed in Equation (25).

$$\dot{C}_Q + \dot{C}_1 + \dot{Z}_{re} = \dot{C}_2 \quad (25)$$

where $\dot{C}_Q$-the cost stream ($/h) at point 1 is due to the electrical power requirements W_{elec} in the reactor component, and $\dot{C}_1$-the cost of the waste plastics material is zero (0). Subscripts such as re-represent reactor; cr-cracker; dif- diffuser; and cd-condenser.

Cracker cost balance

Similarly, the cost balance for the cracker (Mergenthaler *et al.*, 2016) is expressed as given in Equation (26).

$$\dot{C}_3 + \dot{Z}_{Cr} = \dot{C}_4 \quad (26)$$

Since the same stream links up points 2 and 3, a specific cost is assigned to the streams using the fuel principle as follows in Equation (27).

$$\frac{\dot{C}_2}{\dot{E}_2} = \frac{\dot{C}_3}{\dot{E}_3} \quad (27)$$

Diffuser cost balance

The cost balance for the diffuser (Lazzaretto and Tsatsaronis 2006) is expressed in Equation (28).

$$\dot{C}_5 + \dot{Z}_{dif} = \dot{C}_6 \quad (28)$$

Similarly, since the same stream links up points 4 and 5, a specific cost is assigned to the streams using the fuel principle stated in Equation (29).

$$\frac{\dot{C}_5}{\dot{E}_5} = \frac{\dot{C}_4}{\dot{E}_4} \quad (29)$$

Air condenser cost balance

A similar expression for the cost balance is presented for the air condenser (Gorji *et al.*, 2010) and represented in Equation (30).

$$\dot{C}_7 + \dot{C}_9 + \dot{Z}_{cd} = \dot{C}_8 + \dot{C}_{10} \quad (30)$$

As was the case for the previous components, state points 6 and 7 can be related using the fuel principle shown in Equation (31).

$$\frac{\dot{C}_7}{\dot{E}_7} = \frac{\dot{C}_6}{\dot{E}_6} \quad (31)$$

Cost of exergy destruction of the components

The cost rate of exergy destruction for the components is related to the fuel cost($\dot{C}_F$) and the exergetic destruction ($\dot{E}_D$) of the element as given in Equation (32).

$$\dot{C}_D = \dot{C}_F \dot{E}_D \quad (32)$$

Cost of exergy destruction in the reactor

The exergy destruction cost rate of the rector (Mergenthaler *et al.*, 2016) is indicated in Equation (33).

$$\dot{C}_{D_{re}} = \dot{C}_{F_{re}} \dot{E}_{D_{re}} \quad (33)$$

cost of exergy destruction in the catalytic cracker

The exergy destruction cost rate of the catalytic cracker (Gorji-Bandpy *et al.*, 2010) is stated in Equation (34).

$$\dot{C}_{D_{Cr}} = \dot{C}_{F_{Cr}} \dot{E}_{D_{Cr}} \quad (34)$$

Cost of exergy destruction in the diffuser

The cost of exergy destruction in the diffuser (Açıkkalp *et al.*, 2014) is represented in Equation (35)

$$\dot{C}_{D_{dif}} = \dot{C}_{F_{exp}} \dot{E}_{dif} \quad (35)$$

cost of exergy destruction in the condenser

The cost of exergy destruction in the condenser (Abam *et al.*, 2015) is expressed in Equation (36).

$$\dot{C}_{D_{cd}} = \dot{C}_{F_{cd}} \dot{E}_{D_{cd}} \quad (36)$$

2.5 The exergoeconomic parameters

The exergoeconomic parameters considered were the relative cost difference *r* and exergoeconomic factor *f* (Lazzaretto and Tsatsaronis, 2006). For the k^{th} component, the relative cost difference is indicated in Equation (37).

$$r_k = \frac{c_{p,k} - c_{f,k}}{c_{f,k}} \quad (37)$$

The exergoeconomic factor for the k^{th} component is shown in Equation (38).

$$f_k = \frac{\dot{Z}_k}{\dot{Z}_k + c_{f,k}|\dot{E}_{D,k}|} \quad (38)$$

whereas $\dot{c}_{fk}$ is the cost of the fuel and $\dot{c}_{pk}$ is the cost of the product of a component.

Relative cost difference and the exergoeconomics factor for the reactor

The relative cost difference and the exergoeconomics factor for the reactor (Açıkkalp *et al.*, 2014) are expressed in Equations (39) and (40).

$$r_{re} = \frac{c_{p,re} - c_{f,re}}{c_{f,re}} \quad (39)$$

$$f_{re} = \frac{\dot{Z}_{re}}{\dot{Z}_{re} + c_{f,re}|\dot{E}_{D,re}|} \quad (40)$$

Relative cost difference and exergoeconomic factor for the cracker

The relative cost difference and exergoeconomic factor for the cracker (Mergenthaler *et al.*, 2016) are given by the Equations (41) and (42).

$$r_{cr} = \frac{c_{p,cr} - c_{f,cr}}{c_{f,cr}} \quad (41)$$

$$f_{cr} = \frac{\dot{Z}_{cr}}{\dot{Z}_{cr} + c_{f,cr}|\dot{E}_{D,cr}|} \quad (42)$$

Relative cost difference and exergoeconomics factor for the diffuser

The relative cost difference and exergoeconomics factor for the diffuser (Mortazavi and Mehran, 2017) are presented in Equations (43) and (44).

$$r_{dif} = \frac{c_{p,dif} - c_{f,dif}}{c_{f,dif}} \quad (43)$$

$$f_{dif} = \frac{\dot{Z}_{dif}}{\dot{Z}_{dif} + c_{fdif}|\dot{E}_{D\,dif}|} \quad (44)$$

Relative cost difference and exergoeconomics factor for the air condenser

The relative cost difference and exergoeconomics factor for the air condenser (Gorji-Bandpy *et al.*, 2010) are stated in Equations (45) and (46).

$$r_{cd} = \frac{c_{pcd} - c_{fcd}}{c_{fcd}} \quad (45)$$

$$f_{cd} = \frac{\dot{Z}_{cd}}{\dot{Z}_{cd} + c_{fcd}|\dot{E}_{Dcd}|} \quad (46)$$

The exergy cost balance, investment cost rate, exergy of fuel and exergy of the product of the exergoeconomic analysis for the system components analysis are summarised in Table 2.

Table 2: The exergy cost balance, investment cost rate, exergy of fuel and exergy of the product of the exergoeconomic analysis.

Component	Exergy cost balance	Investment cost rate	Fuel cost	Product Cost
Reactor	$\dot{C}_Q + \dot{C}_1 + \dot{Z}_{re} = \dot{C}_2$	$\dot{Z}_{re}$	$\dot{C}_Q + \dot{C}_1$	$\dot{C}_2$
Cracker	$\dot{C}_3 + \dot{Z}_{cr} = \dot{C}_4$	$\dot{Z}_{cr}$	$\dot{C}_3$	$\dot{C}_4$
Diffuser	$\dot{C}_5 + \dot{Z}_{dif.} = \dot{C}_6$	$\dot{Z}_{dif.}$	$\dot{C}_5$	$\dot{C}_6$
Air condenser	$\dot{C}_7 + \dot{C}_9 + \dot{Z}_{cd} = \dot{C}_8 + \dot{C}_{10}$	$\dot{Z}_{cd}$	$\dot{C}_7 + \dot{C}_9$	$\dot{C}_8 + \dot{C}_{10}$

3. Results and discussion

3.1 Exergy and exergoeconomics analysis

A detailed exergy and exergoeconomics analysis are performed for the waste plastics pyrolysis plant as showed in Fig. 2, and their results were plotted in the graph as Figs. 3 - 7, while Tables 4 - 6 contained the summary of the results. A system component with higher exergy destruction means that the

component internal losses is higher during working cycles than another component. When a component's exergoeconomics factor is lower it means that the component need improvement and high total cost rate of the component implies the same enhancement of the component. Using a written source code in EES, the costs were solved simultaneously to obtain the cost rates at the state points. Thus, the external input into the system has its assigned costs in line with current realities. Accordingly, a national tariff of 40 #/kWh (0.1096 $/kWh), was used to calculate the cost of heat requirement of the heater inside the reactor. The most vital input parameters applied in the exergy and exergoeconomics model equations are the temperatures and pressures respectively. The reactor recorded the highest exergy destruction of 0.4322 kW in the pyrolysis plant. The condenser component has a the lowest exergoeconomics factor of 0.00261 with highest total cost rate of 1.895 $/h. The Table 7, represent the characterization results of the diesel oil from thermoplastics.

3.2 Description of the graphs from exergy analysis

The effect of reactor temperature is demonstrated on the parameters of exergy destruction and efficiency. The effect of reactor temperature is demonstrated on the exergetic destruction in the components and is shown in Fig.3. The exergy destruction in the reactor, the cracker, the diffuser and the condenser increased to 0.4322, 0.3084, 0.1677 and 0.3247(kW), respectively, with the increase in the reactor inlet temperature. Thus, the rise in exergy destruction in these components, especially reactor with the highest value of 0.4322 (kW), was due to significant temperature differences at inlet and outlet states. Hence, when a substantial temperature variation drop is intended in the reactor, relatively low temperatures will be needed to reduce exergy destruction. The exergy destruction in the Açıkkalp *et al.* (2014)'s work is higher as compared to the exergy destruction of this work.

As reactor inlet temperature increased from 310 to 500ºC, the exergetic efficiency of the components: reactor, cracker and diffuser decreased downwardly, as shown in Fig 4. The exergetic efficiencies of the components at 500ºC were 76.2, 71.8, 75.6 and 77.46% for reactor, cracker, diffuser and air condenser, respectively. In Ryan, (2015)'s work, the exergetic efficiency of the reactor was 69.9%, which is lesser than the exergetic efficiency in this work, while Jens *et al.* (2015) obtained the overall exergetic efficiency of the reactor to be 71.2% but still lower than the result of the reactor obtained in this work. On the other hand, the exergy efficiency of the condenser increased upwardly and fell at the temperature of 460ºC. Meaning that higher oil yield is better achieved at low temperature.

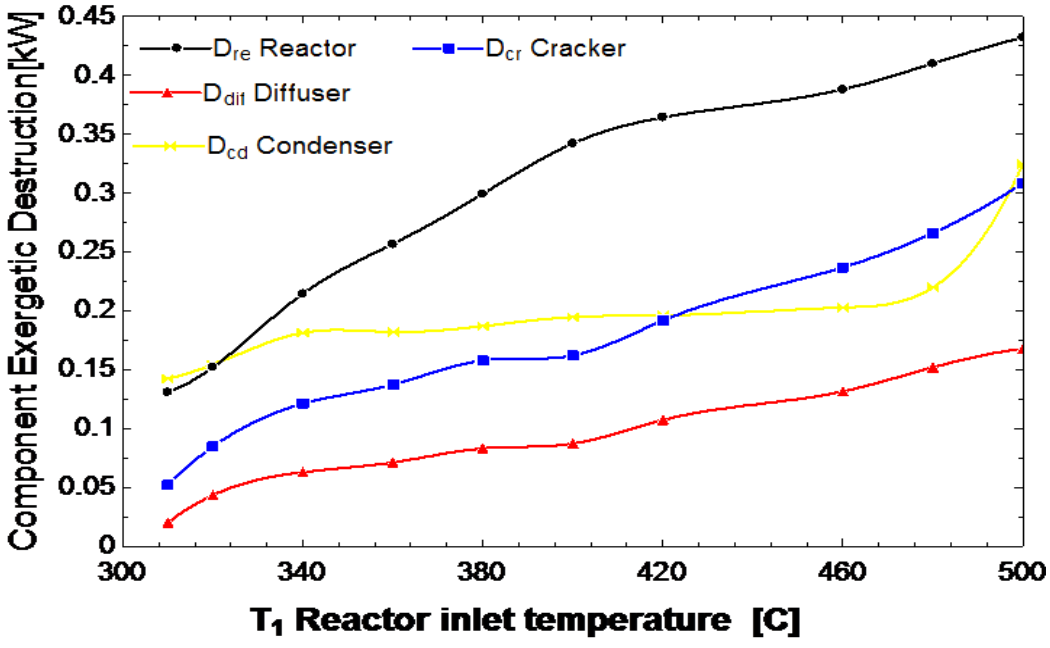

Fig.3: Effect of reactor temperature on component exergetic destruction

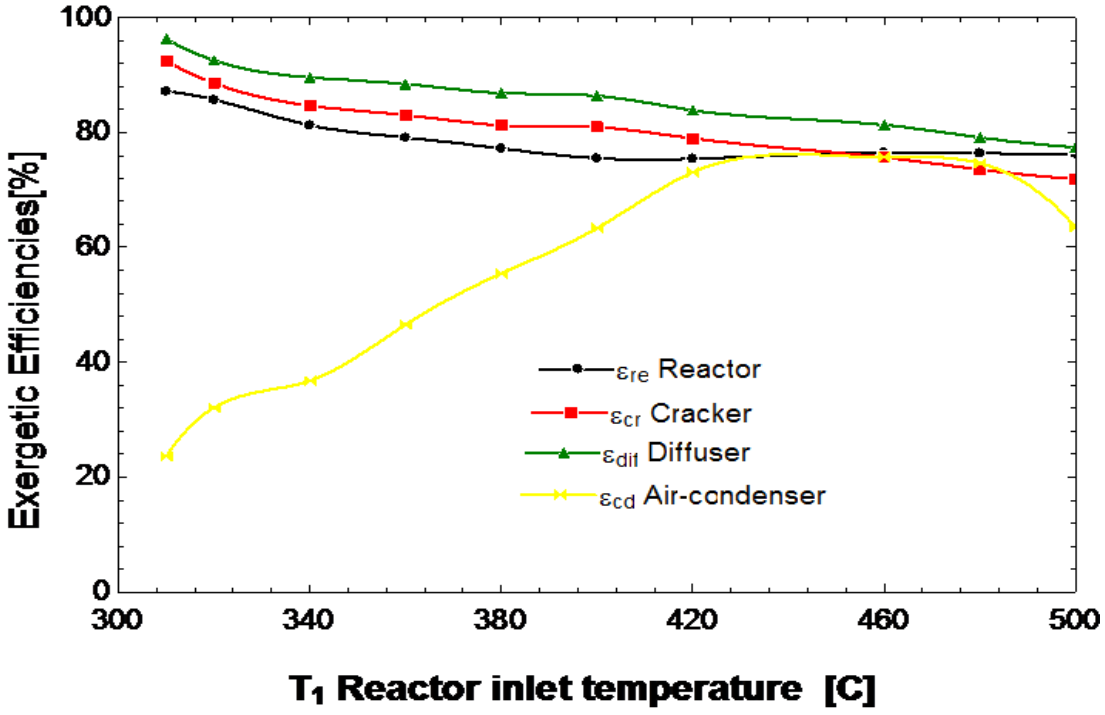

Fig. 4: Effect of reactor inlet temperature on components exergetic efficiencies

3.3 Description of the graphs from exergoeconomics analysis results

The description of the graphs from exergoeconomics results are presented in Figs. 5 - 7. Fig.5 shows the relationship between the reactor inlet temperature and the cost of exergy destruction. The reactor inlet temperature increases also resulted in a corresponding rise in the cost of exergy destruction. This increase was due to the linear relationship between the cost of fuel and exergy destruction, which denotes cost arising from destructions. In fact, between reactor inlet temperatures of 320 to 500 ^{o}C, the cost of exergy destruction increased to 0.07797, 0.4057, 0.3707, and 1.095$/h (38.985, 202.85, 185.35 and 547.5 #/h) for the reactor, the cracker, the diffuser, and the condenser respectively. In addition, the graph suggests that within reactor inlet temperature range of 320 to 460 ^{o}C, the cost of producing diesel oil is meagre, while above 460 ^{o}C, the cost of production increased very high in the condenser, as evident in Fig.4. In general, the graph revealed that producing petroleum products at moderate reaction pyrolysis temperatures (310-460^{o}C) can be achieved by introducing catalysts (iron/silica/zeolite) in liquid/vapour phase contacts, as depicted by Istadi (2010); Rajendra 2017).

Fig. 6 is the graph of inlet temperature on the total cost rate of the plant. The total cost rate of the components increased as inlet temperature increased. The cost rate of the reactor, cracker, diffuser and condenser were 1.578, 0.7057, 0.6707 and 1.895 ($/h), respectively. The condenser had the highest cost rate and emerged as the component with the most increased operating cost and thus needs improving. However, the condenser will be enhanced if the investment cost rate and exergy destruction can be reduced. However, similar findings were realized by Vuckovic *et al.* (2012).

Fig. 7 is the effect of reactor inlet temperature on the exergoeconomics factor of the pyrolysis plant. The exergoecnomics factor decreases as inlet reactor temperature increased. The exergoecnomics aspect of the components plant were 0.06477, 0.00266, 0.00291 and 0.00262(%) for the reactor, cracker, diffuser and condenser, respectively. It can be seen from the fig. 7, above; the condenser had the lowest exergoecnomics factor. If the exergy destruction of the condenser can be reduced, then the condenser will be improved. Similar results can be seen in Mergenthaler *et al.* (2016).

Table 3 represent thermodynamic state points of the waste plastics pyrolysis plant. The inlet and exit temperatures, pressures, exergy stream and enthalpy of state points are presented at various state points. From Table 3, it was revealed that the exergy stream at point 1 of 712 (kJ/kg) reduces as heat flows across the components point to 98.28 (kJ/kg) at point 8. It suggests internal losses in parts and pipelines since the plant has only one source of heat

energy. Furthermore, the enthalpies reduce too from state point 1-8 of the plant components.

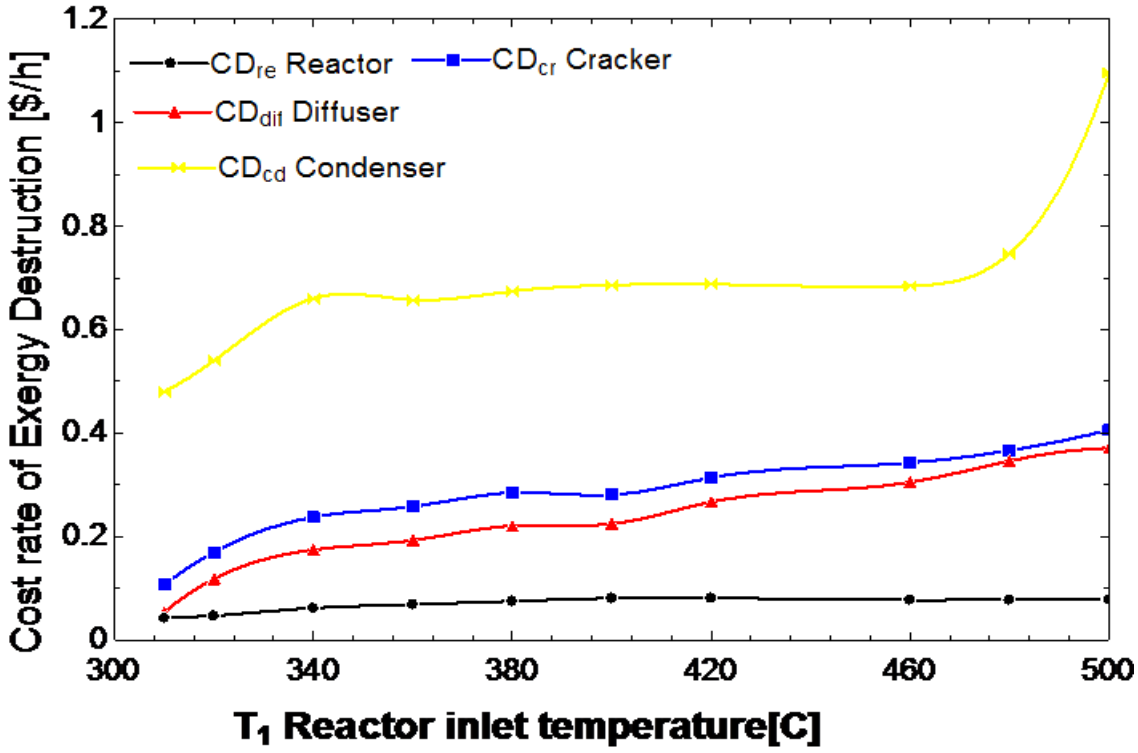

Fig. 5: Effect of reactor inlet temperature on the component cost of exegetic destruction

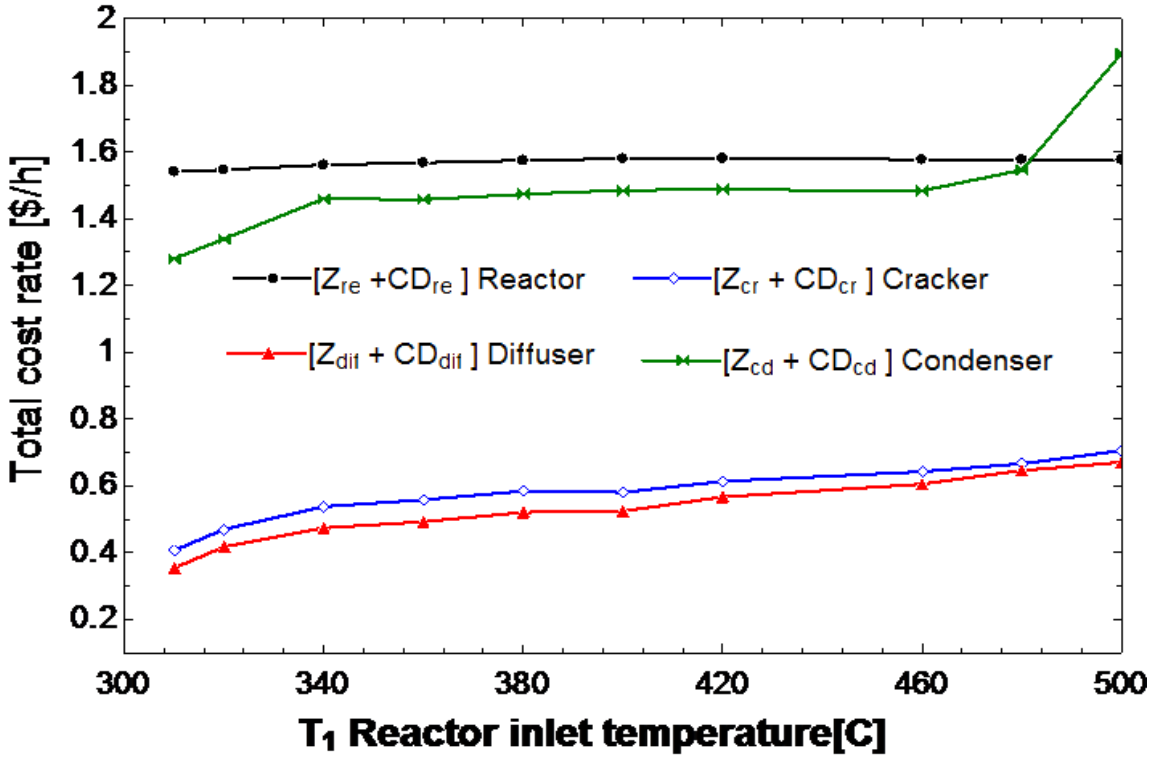

Fig. 6: The effect of reactor inlet temperature on total cost rate of the plant

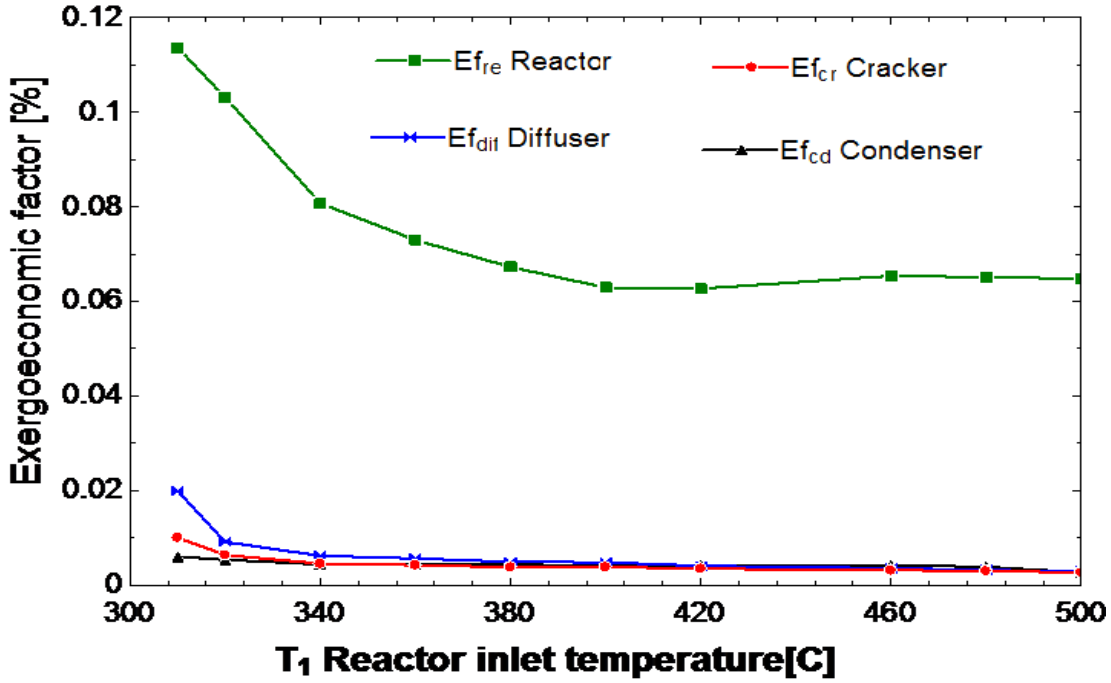

Fig. 7: The effect of reactor inlet temperature on exergoeconomic factors

Table 3: Thermodynamic state points

State Points	T (°C)	Pressure (bar)	Exergy stream (kJ/kg)	Enthalpy of state points (kJ/kg)
1	500	2.5	712	878.5
2	400	2.47	543.1	702.8
3	330	2.45	428.1	579.8
4	255	2.44	308.1	448
5	244	2.43	290.7	428
6	202	2.42	225.1	354.9
7	202	2.41	225.1	354.9
8	116	2.38	98.28	203.8
9	25	2.65	6.9	43.93
10	150	2.62	87.43	263.6

3.4 The interpretation of the exergoeconomics results

The summary of the state points costs of the exergoeconomics results are presented in Table 4 - 6. From Table 4, the cost was calculated based on the heater's heat requirements, which was determined in design analysis to be 3 kW at point 1. Accordingly, taking a national tariff of 40 #/kWh (0.1096 $/kWh), the cost of heat requirement of the heater was approximated to 0.3288 ($/h). Therefore, it can be observed that the cost of heat flows from one component to another increased. Consequently, the cost of condensation of liquid oil at point 8 (2.744 $/h) was higher than other components of the plant.

Table 5 contains the summary of exergy related cost of the plant components in terms of fuel, product cost, exergy destruction, and exergy destruction. From Table 5, the exergy destruction rate in the component is directly related to both the temperature and pressure drops. Consequently, the highest destruction in the system was computed as 0.4322 (kW) in the reactor due to a high-temperature reduction of 100 (°C). This is because most of the heat generated in the reactor was dissipated as heat before the stream exits to the

cracker. Additionally, the cracker observed further destructions at 0.3084 (kW) following a 75 (°C) temperature drop. The pressure drops, however, were negligible due to the size of the plant.

Furthermore, Table 5, also shows the cost of destruction for the components. The cost of destruction was directly related to the cost of the fuel. The condenser had the highest cost of energy at 2.509 ($/GJ) in the plant. Since the fuel cost is related to the exergy destruction, the condenser component invariably emerged with the highest exergy destruction cost rate of 1.095 ($/h). This implies that the heat in this component was dissipated to the ambient and forced through by a high-capacity fan. The results of Table 4 also suggested improvement in the method of condensation of the pyrolysis plant. It also meant that the cost of producing petroleum products in the condenser was higher than the other components of the same plant.

Table 4: Summary of state points cost

State Points	Cost ($/h)	Mass flow rate (kg/s)	Exergy stream(e_k) (kJ/kg)	Exergy flows(E_k) (kW)
1	0.3288	0.00256	712	1.8227
2	1.829	0.00256	543.1	1.3903
3	1.443	0.00256	428.1	1.09593
4	1.743	0.00256	308.1	0.7887
5	1.644	0.00256	290.7	0.7441
6	1.944	0.00256	225.1	0.5762
7	1.944	0.00256	225.1	0.5762
8	2.744	0.00256	98.28	0.2515
9	0.0787	0.018	6.9	0.1242
10	0.2788	0.018	87.43	1.5737

Table 5: Summary of exergy-related cost of plant components

Components	$\dot{C}_F$ [$/GJ]	$\dot{C}_P$ [$/GJ]	$\dot{E}_D$ [kW]	$\dot{C}_D$ [$/h]
Reactor	0.2188	0.9353	**0.4322**	0.07797
Cracker	0.9353	1.657	0.3084	0.4057
Diffuser	1.657	2.509	0.1677	0.3707
Air Condenser	2.509	8.008	0.3247	**1.095**

Table 6: The total cost rates and exergoeconomics factors of the plant

Component	$\dot{Z}$ **($/h)**	$\dot{Z} + \dot{C}_D$ **($/h)**	f	r
Reactor	1.5	**1.578**	0.06477	6.291
Cracker	0.3	0.7057	0.00266	0.6803
Diffuser	0.3	0.6707	0.00291	0.5266
Air Condenser	0.8	**1.895**	0.00261	2.233

From the exergoeconomics viewpoint, the most critical system components are those with the highest sum of the cost rate.($\dot{Z} + \dot{C}_D$). The cost rate of 1.578 $/h in the reactor component was the second component with the highest cost rate after the condenser. Not only that, but the reactor also had the highest relative cost difference of 6.291. It suggests that the reactor requires improvement. For example, the temperature difference between state points in the component can be reduced to improve efficiency. In addition, reducing the capital investment cost can also reduce the total cost rate in the reactor component.

The catalytic cracker and the diffuser have a low-cost rate of 0.7057 and 0.6707$/h, respectively, requiring no further improvement. On the other hand, the air-condenser had the highest total cost rate of 1.895 $/h with a low exergoeconomics factor of 0.00261. Consequently, this suggests that the cost of exergy destruction of the condenser dominated

the plant. Interestingly, this result aligns with Table 4.3 on values of component cost rate of exergy destruction. Nevertheless, since the condenser had the highest value of the cost rate and a low exergoeconomics factor, it is still appropriate to consider reducing the exergetic destruction and the associated investment cost rate, to improve the condenser efficiency. Thus, the exergetic efficiency of the condenser should be improved, and this can be achieved by improving the method of dissipating heat in this component.

Table 7 is the characterization of the diesel oil from the waste pyrolysis plant. The laboratory test was conducted in the Principal Laboratory Technologist at the National Root Crops Research Institute Umudike Abia State Nigeria. The fuel samples were tested to determine the fuel characterization parameters according to the ASTM 675 for diesel oil and light fuel oil quality assurance standard test in Table 7. The colour had no direct influence on the functioning of an engine but only indicates the quality of the samples. The density is a fundamental physical property that can be used (in addition to other properties) to characterize the light and heavy fraction of fuel. A density in the range 810-890 (kg/m^3) for diesel ensured good running of the engine in this study, as evident in Table 7. Furthermore, it was found that the density of diesel oil was by the limitation standards of ASTM D4052. One of the properties to be considered in assessing the overall risk of fuel flammability is the flashpoint. This is the highest temperature at which a fuel can be handled without risk of explosion. Consequently, the flesh points observed for diesel fuel met the ASTM specifications for all diesel products. In addition, the pour point of a fuel is the lowest temperature at which fuel freezes. Therefore, this value determines the fuel heating conditions to be considered in cold weather by appropriate additives. Also, the viscosity was performed at 40^{o}C and conformed to national standards of ASTM D445 requirement for diesel fuel oil grade D2.

In summary, the results from the laboratory revealed that liquid oil with reactor inlet temperatures of 310,360,400 and 460^{o}C have close results with standard diesel oil. But stressed that the diesel oil (AGO) with a reactor inlet temperature of 360^{o}C was the best and had the same oil quality as regular diesel oil.

Table 7: Characterization of the diesel oil from the plant

Test property	**Test method**	**Diesel**	**Standard Limits**
Flashpoint ^{0}C	ASTM D93	76	>55
Pour point ^{0}C	ASTM D97	-10.80	-32
Boiling point ^{0}C	Oil weathering system	358	369
Self-ignition temp ^{0}C	ASTM D97	711	725
Lower heating value MJ/kg	ASTM D240	44.8	45.9
Density at 40 ^{0}C (kg/m^3)	ASTM D4052	837	810 – 890
Viscosity at 40^{0}C ($N.s/m^2$)	ASTM D445	3.6	2.0 -4.5
Sulfur content, %	ASTM D5453	0.23	0.16
Saturates content Vol. %	ASTM D2007	77.3	75.3 –79.3
Specific gravity, 15^{o}C	ASTM4052	0.88	0.82 -0.95
Ash content % mass	ASTM D482	0.007	MAX 0.01
Water content % volume	ASTM D95	0.20	0 – 0.50

4. Conclusion

The waste plastics pyrolysis plant was subjected to energy and exergoeconomics analysis to identify thermal and cost-related system improvements. In addition, performance analysis was made, and several key parameters were investigated on the thermal and exergoeconomics performance of the plant. The plant's reactor, catalytic cracker, diffuser, and air-condenser exergy efficiencies were 76.29, 71.89, 77.46 and 63.49%, respectively. The reactor components of the plant had the highest exergy destruction flow rate of 0.4322 kW. The air-condenser part had the highest value of exergy destruction cost rate of 1.095($/h) and total cost rate of 1.895($/h) in the plant. This suggests that condensation in the plant to produce oil should be improved by enhancing the method of dissipating heat in this component.

References

Abam, F.I. Ohunakin, O.S. Nwankwojike, B.O. and Ekwe, E.B. (2012) End-use energy utilization efficiency of Nigerian residential sector. Frontiers in energy, 8(3): 322-334.

Açıkkalp, E. Haydar, A. and Arif, H. (2014) The advanced exergy analysis of an electricity generating facility using natural gas. Energy Conversion and Management, 82:146–153.

Balli, O. (2017) Advanced exergy analysis to evaluate the performance of a military aircraft turbojet engine (TJE) with an afterburner system: Splitting exergy destruction into unavoidable/avoidable and endogenous/exogenous. Applied Thermal Engineering, 111:152–169.

Darabi, M. Mohammadiun, H. and Mohammadiun, M. (2015) Advanced exergy analysis of distillation tower and simulation and optimization by Hysys. International Journal of Scientific World, 3(1):163-177.

Erbay, Z. and Hepbasli, A. (2014) Application of conventional and advanced exergy analysis to evaluate the performance of a ground-source heat pump (GSHP) dryer used in food drying. Energy Conversion and Management, 78:499–507.

Eugene, P. (2013) Energy from Switchgrass: Bio-Mass Conversion Analysis. B.S., Swarthmore, College Department of Engineering.

Galindo, J., Ruiz, S., Dolz, V. and Royo-Pascual, L. (2016) Advanced exergy analysis for a bottoming organic Rankine cycle coupled to an internal combustion engine. Energy Conversion and Management, 126:217–227.

Gorji-Bandpy M., Goodarzian, H. and Biglari, M. (2010) The Cost-Effective Analysis of a Gas Turbine Power Plant. Energy Sources Part B, (4):348-358.

Istadi, L. Lugman, B. and Suherman, S. (2010) Optimization of Temperature and Catalyst Weight for Plastic Cracking to fuels using Response Surface Methodology. Bulletin of Chemical Reaction Engineering & Catalysis, 5(2): 103-111.

Jens, F.P. Fontina, P. and Javier, D. (2015) Exergetic analysis of a fast pyrolysis process for bio-oil production. Fuel Processing Technology, 119:245–255.

Kelly, S. Tsatsaronis, G. and Morosuk, T. (2009) Advanced exergetic analysis: Approaches for splitting the exergy destruction into endogenous and exogenous parts. Energy, vol. 34, pp. 384–391.

Koroglu, T. and Sogut, O.S. (2017) Advanced exergy analysis of an organic Rankine cycle waste heat recovery system of a marine power plant. Journal of Thermal Engineering, 3(2): 1136-1148.

Lazzaretto, A. and Tsatsaronis G. (2006). A systematic and general methodology for calculating efficiencies and costs in thermal systems. Energy, 31(8):1257-1289.

Mergenthaler, P., Schinkel, A. and Tsatsaronis, G. (2016) Application of exergoeconomic, exergoenvironmental and advanced exergy analysis on Carbon Black production. Proceedings of Ecos 2016.

Morosuk, T. and Tsatsaronis, G. (2015) Advanced exergy analysis based on the parametric study of the regasification of LNG integrated into an air separation process. Proceedings of the ASME 2015 International Mechanical Engineering Congress and Exposition IMECE 2015, pgs. 1-9.

Morosuk, T., Tsatsaronis, G. and Schult, M. (2013) Conventional and Advanced Exergetic Analysis: Theory and Application. Arabian Journal of Science and Engineering, 38:395–404.

Mosaffa, A.H., Garousi, L., Infante, C.A. and Rosen, M.A. (2014) Advanced exergy analysis of an air conditioning system incorporating thermal energy storage, 77, 945-952.

Rajendra, P.M. (2017) Design and Development of Fixed-Bed Type Fast Pyrolysis Unit.

Trindade, A.B., José, C.E., Aldemar, M., Dimas, J., Electo E., Maria, L. and Oscar, A. (2018) Advanced exergy analysis and environmental assessment of the steam cycle of an incineration system of municipal solid waste with energy recovery. Energy Conversion and Management, 157: 195–214.

Vuckovic, G.D., Stojiljkovic, M.M. and Vukic, M.V. (2015) First and second level of exergy destruction splitting in advanced exergy analysis for an existing boiler. Energy Conversion and Management, 104 8–16.

Wang, L., Yang, Y., Morosuk, T. and Tsatsaronis, G. (2012) Advanced Thermodynamic Analysis and Evaluation of a Supercritical Power Plant. Energies, 5(6): 1850-1863.